Energy & Buildings 360 (2026) 117391

Contents lists available at ScienceDirect

Energy & Buildings

journal homepage: www.elsevier.com/locate/enb

One-year performance assessment of a passive house container-based prototype: Indoor comfort and energy use

Adeline Rezeau *, Beatriz Rodríguez-Soria, Miguel Ángel García-García

CUD – University Defence Centre, Universidad de Zaragoza, Academia General Militar, Crtra. Huesca s/n, 50090 Zaragoza, Spain

ARTICLE INFO

Keywords:
Living container
Passivhaus standard
Energy efficiency
Thermal comfort
Indoor environmental quality
Military bases

ABSTRACT

This study provides new insights into the energy and environmental performance of buildings constructed from shipping containers, which are widely used worldwide for temporary accommodation in both civilian and military contexts. Such structures often exhibit poor thermal performance and inadequate indoor air quality, as they are typically designed for short-term use despite being occupied for extended periods in refugee camps or military peacekeeping missions. This mismatch between design assumptions and real use leads to suboptimal comfort, high energy demand, and increased operational costs.

This research presents a passive, modular, habitable and demountable prototype specifically designed for deployment in Antarctica and adaptable to remote military bases elsewhere. The prototype was developed in accordance with the Passivhaus standard, NATO environmental protection requirements, and the Protocol on Environmental Protection to the Antarctic Treaty. Before its installation at an Antarctica research station, the module was monitored over one year at a military base in Zaragoza, Spain. Indoor environmental conditions (air temperature, relative humidity, and CO_2) and energy consumption for ventilation and air conditioning were assessed.

Results show that the prototype maintained stable indoor temperatures during winter, avoiding cold-wall and vertical stratification effects, while CO_2 concentrations confirmed consistently adequate air renovation. In summer, acceptable indoor conditions were maintained on most days, although significant overheating occurred during two heatwaves. Overall, the annual energy consumption for heating and cooling was 33.9 kWh/m^2, representing an 87 % reduction compared with conventional containerised units previously monitored by the authors.

1. Introduction

Containerised housing have become a versatile solution for diverse accommodation needs, ranging from civilian and post-disaster settlements to military bases and construction camps [1,2]. Its appeal lies in modularity, prefabrication, structural robustness, and ease of transport by ship, rail, air, or truck [3]. Standardised manufacturing ensures reusability and rapid deployment, while different configurations allow adaptable layouts. The most common units are 20-foot and 40-foot containers, typically composed of steel profiles with corrugated steel panels or insulated sandwich systems to enhance thermal performance.

In post-disasters contexts, reconstruction is generally structured in phases, from emergency shelter to temporary housing and permanent rebuilding. Container-based solutions are widely used as transitional dwellings, balancing rapid deployment with longer-term sustainability goals. However, as noted by Zhang et al. [4], such projects must reconcile urgent short-term needs with sustainable community development. Atmaca and Atmaca [5] further emphasised that the demand for such temporary housing has steadily increased in recent decades, driven by immigration and the growing frequency of natural disasters, a trend expected to continue in the future.

Similar challenges arise in military contexts, where containerised

Abbreviations: ATEX, ATmoshpere Explosive; CSC, Convention for Safe Containers; DHW, Domestic Hot Water; EN, European Norm; EPBD, Energy Performance of Building Directive; HVAC, Heating, Ventilation and Air Conditioning; GSM, Global System for Mobile Communications; MR, Module Room; NTC, Negative Temperature Coefficient; n_{50}, Airtightness at 50 Pa [1/h]; PHI, Passive House Institute; PHPP, Passive House Planning Package; q_{E50}, Airtightness per envelope area at 50 Pa [m^3/h.m^2]; RH, Relative Humidity; XPS, Extruded Polystyrene; ZEM, Zero Energy Module.

* Corresponding author at: CUD – University Defence Centre, General Military Academy, Crtra. Huesca s/n, 50090 Zaragoza Spain.
E-mail address: arezeau@unizar.es (A. Rezeau).

https://doi.org/10.1016/j.enbuild.2026.117391
Received 9 January 2026; Received in revised form 4 March 2026; Accepted 26 March 2026
Available online 28 March 2026

units support rapidly deployable operational bases [6]. Although technologies implemented in peacekeeping missions are typically selected according to the expected duration of the mission (six to twelve months), actual deployments often extend to several years. This discrepancy discourages investment in high-performance envelopes and energy-efficient systems, resulting in prolonged operation under suboptimal thermal conditions and elevated energy demand, with associated economic, logistical, and environmental impacts. For example, at the Spanish base *Ruy González de Clavijo* during the ISAF mission in Afghanistan, nearly 80 % of the energy consumed in living containers was dedicated to heating and cooling, with the remainder used primarily for lighting [7]. Beyond the energy penalty, these deficiencies also compromise indoor air quality and occupant comfort, as it has been shown by previous studies [1,8,9].

Similarly, in terms of energy consumption for space heating, Atmaca et al. [5] reported an annual energy consumption of 20140 MJ for heating a container CH20 (5 × 4 m), equivalent to 280 kWh/m^2 per year. This value is more than three times the average energy consumption for space heating in EU-27 households [10] and more than 20 time higher than thresholds set by high efficiency standards such as Passivhaus [11]. Previous studies by the authors further confirmed the large potential for improvement. For instance, experimental data collected at the *Gabriel de Castilla* research station in the Antarctica showed that energy consumption for space heating in a containerised-based building was 27 kWh/m^2 over a four-week monitoring period [9]. Likewise, at the *Miguel de Cervantes* military base in Lebanon, the annual energy consumption for air conditioning (both heating and cooling) in living containers was estimated to be between 140 and 264 kWh/m^2 per year, depending on usage patterns and occupancy [8].

These high consumption levels, combined with the continued reliance on fossil fuels for supply, remain inconsistent with the targets established in recent years by governments and international institutions. At the European level, the revised Energy Performance of Buildings Directive (EPBD) 2024/1275 [12] requires Member States to achieve cumulative end-use energy savings in order to progress towards a zero-emission building stock by 2050. However, where a building is initially designated as temporary, minimum energy performance requirements are not mandatory and are left to the discretion of each country or owner. According to Article 5.3 of the revised EPBD 2024/1275 [12], energy performance obligations do not apply to temporary buildings with a planned use of two years or less.

Similarly, exemptions exist for buildings owned or operated by the armed forces and serving national defence purposes, for which Member States may determine whether and how energy performance requirements are implemented. In this context, the NATO Military Committee approved in 2011 the document “MC-469: NATO Principles and Military Policy for Environmental Protection”, which defines environmental protection responsibilities for NATO member states engaged in Alliance military activities. Building upon this framework, NATO has developed common environmental and energy-related procedures through Standardization Agreement (STANAG), including the Allied Joint Environmental Protection Publications (AJEPP). These instruments are generally implemented on a voluntary basis, allowing each nation to adopt them according to national priorities.

This regulatory flexibility, combined with the continued use of low-performing containerised solutions across civilian, military, and humanitarian contexts, highlights the need for innovative design approaches capable of ensuring high-energy efficiency and adequate indoor environmental quality, even when buildings are formally classified as temporary.

Most existing research on container-based buildings relies on numerical modelling and simulation to evaluate energy performance. Elrayies [13] compared four insulation materials for a 20-foot container and found that spray polyurethane achieved the best thermal performance, followed by straw. Similarly, Da Costa et al. [14] assessed internal insulation strategies using Building Information Modeling (BIM) and Building Energy Simulation (BES) tools, reporting significant energy savings, with mineral wool offering the best long-term performance. Shen et al. [2] and Koke et al. [15] proposed passive design strategies for Nearly Zero-Energy Container Buildings (NZECBs), recommending advanced envelope solutions such as vacuum insulation panels and phase-change materials, although their feasibility for temporary housing remains uncertain. In subtropical climates, Suo et al. [16] demonstrated through EnergyPlus simulations that cooling demand can be substantially reduced by limiting air infiltration and increasing insulation thickness. Schiavoni et al. [17] also reported promising simulated results for a mix of polyurethane foam insulation layers with a 50-mm vacuum insulation panel, with average HVAC electricity consumption of 44 kWh/m^2·year in the Perugia region (Italy). These findings are promising, although their technical and economic feasibility has not yet been experimentally validated.

Previous research has also examined the energy and environmental performance of container-based housing through life cycle assessment and life cycle costing analyses [18–22]. Nevertheless, only a limited number of studies have conducted experimental investigations into the implementation of energy-efficient solutions in containerised buildings intended for temporary use. Two notable exceptions are the container house with passive technologies tested by Wei et al. [23], and the off-grid container unit developed by Kristiansen et al. [24]. In the first, the authors showed that integrating passive measures such as enhanced insulation and air tightness reduced energy consumption by up to 72 % compared with a conventional container unit. In the second study, Kristiansen et al. [24] reported a 40 % reduction in heating energy use after installing vacuum insulation panels. Despite their excellent insulation performance, these panels present several drawbacks, including mechanical fragility, high cost and uncertain long-term durability. Taken together, these limitations make vacuum insulation panels unsuitable for container-based construction intended for temporary use, particularly in military applications.

Overall, a substantial research gap remains in the experimental validation of energy-saving strategies using real container prototypes monitored over representative periods. The present study addresses this gap by evaluating the energy performance of the so-called *Zero Energy Module* (ZEM), a nearly-zero energy, transportable, demountable and habitable prototype. Although originally conceived for remote military bases, its design principles are applicable to other temporary housing needs, such as refugee camps, emergency classrooms or post-disaster dwellings.

The ZEM aims to deliver a self-sufficient building solution meeting Passivhaus standard, integrating high energy-efficiency measures with on-site renewable generation and hybrid energy storage (batteries and hydrogen). The concept is founded on a simple yet often overlooked principle: “the best energy is the one not consumed”, prioritising demand reduction before renewable supply. Co-financed under the EU LIFE programme, the prototype was certified in 2025 as a “Low Energy Building” by the Passivhaus Institut (Darmstadt, Germany).

This paper focuses specifically on the demand-side performance of the prototype. We describe how Passivhaus and NATO environmental protection standards were implemented in the ZEM, evaluate its monitored performance over one year in terms of thermal comfort and energy consumption for heating, ventilation and air conditioning (HVAC). The analysis of on-site renewable generation and the overall annual energy balance will be addressed in future work.

2. Materials and method

2.1. *ZEM* prototype description

The ZEM prototype was developed to demonstrate the feasibility of applying the Passivhaus standard to a modular, transportable, and demountable construction system based on shipping containers. High-Cube 20-foot containers were selected, as they hold international CSC

certification for worldwide transport and offer a structural configuration that allow integrating a ceiling void suitable for routing technical systems such as air-conditioning ducts and electrical cabling.

As detailed in a previous study by the authors [8], the prototype complies with the requirements of the EPBD, the Passivhaus standard, and relevant NATO standards (AJEPP-2 and AJEPP-4) [25,26]. In addition, it was specifically designed for future deployment at the *Gabriel de Castilla* Antarctic research station, which is managed by the Spanish Army and where the authors previously carried out research on the energy performance and thermal envelope characteristics of several buildings [9]. Consequently, the material selection for the ZEM module was carried out in accordance with the requirements of the Protocol on Environmental Protection to the Antarctic Treaty [27,28], ensuring compliance with strict environment standards while also guaranteeing adequate performance and, hence, its *Passivhaus* certification, under the extreme climatic conditions of the polar island.

The complete ZEM prototype consists of four High-Cube 20-foot containers assembled to create a total usable floor area of 62 m^2, with a projected building footprint of 83.4 m^2. This space is functionally divided into three zones: habitable rooms, which occupy 37.5 m^2 (12.5 m^2 per container or room); facilities and hydrogen production areas, accounting for 12.6 m^2; and a central core of 11.9 m^2 that houses the shower and toilet facilities along with two sinks. The overall layout is shown in Fig. 1, which also indicates the placement of the sensors used in this first monitoring campaign (see Table 3), while Table 1 presents the main building characteristics.

The containers feature a rigid, stackable chassis structure that has been adapted to eliminate thermal bridges. Basic insulation is provided by 10 cm of high-density mineral wool integrated into removable chassis enclosure panels. Externally, each container is equipped with a thermal skin system consisting of 30 cm of interlocking extruded polystyrene (XPS) panels, assembled using a tongue-and-groove technique. These insulation thicknesses were defined to satisfy Passivhaus criteria for the prototype's intended deployment at the Antarctic research station, a polar environment with a mean annual temperature of approximately −1.2 °C and harsh winds carrying moisture and abrasive pyroclastic particles [9]. This envelope also incorporates an airtight system designed to prevent uncontrolled air infiltration and drastically reduce thermal bridges. The same XPS system, selected for its high mechanical strength, was applied to insulate the foundation, ensuring a hermetic and thermally stable base (see Fig. 2 – left). The constructive method used in the ZEM prototype is currently under patent review.

The envelope design prioritises airtightness and thermal performance. Opaque enclosures are continuously insulated to eliminate thermal bridges, while the airtight layer is uninterrupted and sealed with durable tapes and expanding sealants resistant to long-term degradation. The exterior cladding is stainless steel, chosen for its exceptional resistance to the harsh environmental conditions of Antarctica, including extreme cold, high winds, and saline exposure. The total wall thickness is 51.1 cm and is consistent across the roof, floor, and vertical walls. The resulting thermal transmittance (U-values) ranges 0.072–0.073 W/m^2K, depending on orientation and contact with exterior air or ground. These values are well below the requirements of the Spanish Technical Building Code [29] and fall within the lower range of average U-Values reported for nZEB buildings in European Member States [30]. Further details on thermal conductivity and thickness of each material layer composing the ZEM envelope are provided in the Appendix (Table A.1).

A glazed door (1.04 x 2.20 m) serves as the sole entrance to the module, complemented by three windows (0.85 x 2.0 m) positioned on the lateral façades, one per container except in the facility-hydrogen room. The window-to-wall ratio was optimized to balance adequate natural lighting with structural robustness for transport and on-site assembly. Moreover, each window is integrated into the prefabricated vertical insulation panel as part of a unified structural assembly. Both the door and windows are high-performance, PHI-certified elements with triple glazing, double low-emissivity coatings, krypton gas infill, and spacer bars incorporating desiccant materials (WERU MEGATHERM 4*/12A/4/12A/4* with WERU AFINO PVC frame), designed to prevent condensation and enhance thermal performance. Their U_w value is 0.735 W/m^2K. It is noteworthy that the windows are fixed, as required by the specifications for the module's intended use at the Antarctic research station, with indoor ventilation provided exclusively through a mechanically controlled system.

As the construction is intended to operate autonomously in remote areas, it integrates an self-sufficient energy system combining multiple renewable sources. Electricity is generated by solar photovoltaic modules (5.4 kWp) and a small wind turbine (3 kW). Energy storage relies on lithium-ion batteries ($LiFePO_4$ with 14.4 kWh), complemented by a hydrogen-based system for generation, storage and utilization. Air conditioning is provided by air supplied by a mechanical ventilation system with an enthalpy recovery unit. The required temperature increase at the exhaust of the recovery unit is achieved by an aerothermal energy system. For this purpose, a Pichler PKOM4 classic unit was installed, comprising two parallel heat pumps that supply both air conditioning and domestic hot water (DHW), with maximum capacities of 1.3 and 1.6 kW, respectively. This unit was selected for its high efficiency, reporting coefficients of performance (COP) of up to 6.8 for heating and 4.2 for cooling according to the manufacturer's technical specifications [31], as well as its ability to supply both HVAC and DHW in a compact system, without the need of an outdoor unit. These features are particularly advantageous for Antarctic deployment, where extreme weather would significantly degrade external equipment performance, and it also avoids the need to drill into the building envelope.

To ensure a relevant demonstration under realistic operating conditions representative of Army bases, the prototype was deployed and tested at Sapper Battalion I in Zaragoza, Spain, where the first monitoring campaign was conducted (see Fig. 2). At this site, the module was evaluated and adjusted as needed to optimise the performance of the energy management systems. The prototype layout is shown in Fig. 1, including its orientation with respect to cardinal directions for the subsequent analysis of the measured data. A deviation of 23° from the true north–south direction axis was recorded. The orientation, acronym and use of each container during the first demonstration are summarised in the Table 2. In this initial deployment, the prototype accommodated four soldiers, who used the ZEM module as an office.

2.2. Monitoring sensors and methodology

2.2.1. Thermal envelope characterisation

To ensure the ZEM prototype meets the required energy performance and indoor comfort standards, a detailed assessment of its thermal envelope was carried out, focusing on surface temperatures and airtightness. Surface temperatures were continuously monitored in the three module rooms and compared with the corresponding indoor air temperature (see section 2.2.2 and Table 3).

Airtightness tests were conducted using the RETROTEC Blower Door 300 CP DM32 system to quantify air infiltration through the enclosure joints. The procedure followed the specifications of ISO 9972 [32], including a series of pressurisation and depressurisation tests. Several tests iteration were necessary, as the initial n_{50} values exceeded one air change per hour, higher than the threshold anticipated at the design stage. Complementary thermal imaging (with a Testo 868 camera) revealed several air leaks, primarily in the hydrogen room. Consequently, a detailed inspection of all utility line penetration was performed, and design modifications were introduced to the hydrogen emergency extractors, which are triggered in the event of gas detection.

2.2.2. Thermal comfort and indoor air quality

To evaluate the indoor environmental conditions of the ZEM prototype, measurements of air temperature, relative humidity, and CO_2 concentration were taken at various locations within the module.

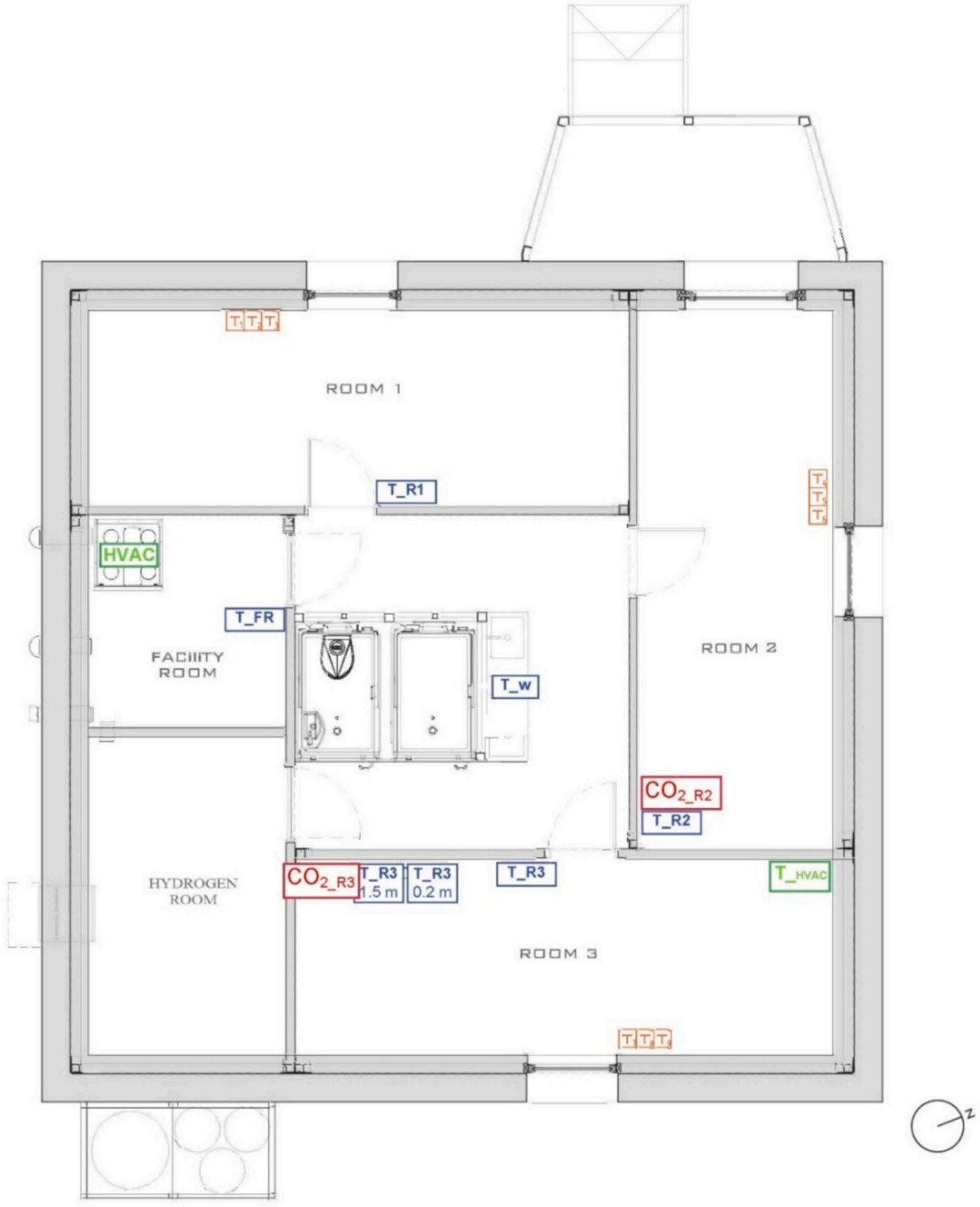

Fig. 1. Layout of the ZEM prototype and location of monitoring sensors.

Table 1
ZEM prototype building characteristics.

External dimensions	Length: 9.13 m; Width: 9.13 m; Height: 4.10 *m*
Useful floor area	61.9 m^2
Treated Floor Area [a]	56.8 m^2
Internal volume	136.2 m^3
Occupancy[b]	4 soldiers working from Monday to Friday: Weekdays 9 am – 3 pm Weekends empty

[a] TFA as defined by the Passive House Planning Package (PHPP) manual, see *Section 3.3* for further details.
[b] The soldiers primarily worked in the module on weekdays, although specific manoeuvres occasionally required them to sleep inside the module for several consecutive days.

Thermal gradients were also assessed, and temperature differences between rooms were analysed with respect to their function and orientation, providing a comprehensive characterisation of indoor comfort conditions. In addition, the authors conducted interviews with the soldiers who worked in the module during the monitoring period to further complement the assessment of environmental comfort.

The sensors and equipment installed in the ZEM prototype include:

- 7 Kintech K308TH temperature sensors, range −30 – 70 °C, accuracy ± 0.3 °C at 20 °C and ± 0.5 °C at −30 – 70 °C.
- 3 of the K308TH sensors include relative humidity sensors, range 0 – 100 %, accuracy ± 3 %.
- 2 dual-channel CO_2 sensors T6615-5 K Telaire, range 0 – 5000 ppm, accuracy ± 75 ppm at 400 – 1000 ppm and ± 10 % of reading at > 1000 ppm.
- 9 encapsulated, self-adhesive NTC Amphenol JS6670 surface temperature sensors, range −30 – 70 °C, accuracy ± 1 °C at 20 °C.
- 1 Kintech Orbit 360 Basic Plus logger (25 channels) with GSM telemetry module.

All measurements were recorded at one-minute intervals and subsequently averaged to hourly values for analysis. Greenwich Mean Time (GMT + 00) is used throughout this article. For surface temperature measurements, three sensors were installed per wall to cover an area of approximately one square meter. Indoor comfort data were compared with outdoor environmental data obtained from a weather station at Zaragoza airport, and accessed through Meteonorm software. The location and nomenclature of all sensors are provided in Fig. 1 and Table 3.

2.2.3. Energy consumption

The energy consumed for both HVAC and DHW purposes was monitored using the built-in software of the Pichler PKOM4 unit. This system also enabled the calculation of specific and seasonal efficiencies for heating and cooling. Electrical energy consumption for ventilation, heating, cooling and DHW was recorded individually, allowing a detailed analysis of the contribution of each system to the overall energy demand. The results obtained are presented in Section 3.3.

3. Results and discussion

3.1. Thermal Envelope Characterization

The measurement of surface temperatures and the blower door test, together with thermographic analysis, enabled the assessment of the condition of the insulation materials and of the connections between the different panels. Table 4 provides the theoretical thermal transmittance values of opaque walls, vertical windows and the glazed door, along with the air infiltration rate measured in the ZEM prototype. These values are compared with the recommended limits established in the Spanish Technical Building Code, specifically in the Basic Document for Energy Saving [29], as well as the criteria of the Passivhaus standard [33]. Both set of values represent recommended thresholds aimed at achieving the mandatory energy performance levels defined by the Energy Performance of Building Directive and the Passivhaus standard, respectively. In addition, Table 4 also includes the strictest national transmittance limits currently in force within the EU Member States, recently reported by Congedo et al. [34]. These limits correspond to the Luxembourg Building code, revised in 2017.

As shown in this table, the substantial thickness of the ZEM wall assembly results in the lowest U-value for opaque elements when compared with all referenced standards. Regarding the windows, the ZEM U-value falls below the strictest limits applied across EU, although it remains slightly above the Passivhaus recommendation for Artic zone. Achieving the latter threshold (0.45 W/m^2K) would have required the use of vacuum glazing, a solution that would have reduced window surface area, and considerably increased both costs and maintenance complexity. In all cases, the greater window U-value of ZEM prototype is effectively compensated by the enhanced insulation of the wall assembly.

During the design phase, linear thermal transmittances (Ψ-values) were calculated using THERM software to ensure that heat losses at thermal bridges remained below the limits recommended by the Passivhaus standard. Conventional container-based constructions typically exhibit significant thermal bridging at corners and panel junctions due to presence of the steel chassis. In contrast, the ZEM design achieves very

Table 2
Orientation, acronym and use of containers during the first demonstration.

Room name		Orientation	Use during Demo
Module Room 1	MR1	Window: West-Northwest (WNW)	Office for 2 soldiers
Module Room 2	MR2	Door: West-Northwest (WNW) Window: North-Northeast (NNE)	Entrance and coffee room
Module Room 3	MR3	Window: East-Southeast (ESE)	Office for 2 soldiers
Facility & Hydrogen Room	FR	No door, no window	–

Fig. 2. ZEM prototype during commissioning (left) and demonstration (right) at the Sapper Battalion I, Zaragoza.

Table 3
Summary of the monitoring sensors and their respective locations within the ZEM prototype.

Sensor location	Ambient Temperature [°C]	Relative Humidity [%]	Wall Temperature [°C]	CO_2 concentration [ppm]
Habitable module – MR1	T_{R1}	–	T_1, T_2, T_3	–
Habitable module – MR2	T_{R2}	RH_{R2}	T_4, T_5, T_6	CO_{2_R2}
Habitable module – MR3	T_{R3}	RH_{R3}	T_7, T_8, T_9	CO_{2_R3}
Habitable module – MR3 (1.5 m)	$T_{R3\_1.5}$	–		–
Habitable module – MR3 (0.2 m)	$T_{R3\_0.2}$	–		–
Facility room	T_{FR}	–		–
Central zone – Bathrooms	T_W	RH_W		–

Table 4
Comparison between threshold and theoretical/measured values of ZEM prototype.

Ref. values / Case study	**U-value opaque envelope (W/m^2K)**	**U-value vertical windows (W/m^2K)**	**n_{50} Air tightness (1/h)**	**q_{E50} Air tightness ($m^3/h.m^2$)** [a]	**Ψ Linear thermal transmittance** [b]
CTE DB-HE [29]	< 0.37 For climatic zone E [c]	< 1.8 For climatic zone E	< 6 For compactness below 2 m^3/m^2	–	–
Strictest EU (national) limits [34]	< 0.13 For external walls	< 0.9 For windows	–	–	–
Passivhaus standard [33]	< 0.09 For artic climate zone < 0.30 For warm-temperate climate zone	< 0.45 For artic climate zone < 1.05 For warm-temperate climate zone	< 0.6 For Classic/Plus/Premium < 1 For Low Energy Demand Building	< 0.6	< 0.01
ZEM prototype [d]	**0.072**	**0.735**	**0.9**	**0.5**	**Max. 0.008**

[a] Airtightness per envelope area.
[b] Linear transmittance coefficient in W/mK.
[c] For each wall in contact with exterior air.
[d] U-values are theoretical, while n_{50} and q_{50} are measured values. Ψ coefficients calculated with THERM software.

low Ψ-values by means of a fully continuous insulation layer that thermally decouples the structural steel from both outdoor and indoor environments.

Respect to air tightness, measurements were conducted using the RETROTEC Blower Door 300 CP DM32 system, as described in Section 2.2.1. Averaging the values obtained under both positive and negative pressures, the ZEM module exhibited 0.98 air changes per hour, at 50 Pa, slightly below the Passivhaus threshold for a "Low Energy Demand Building" [33]. Although the module was initially designed to meet the highest performance criteria ($n_{50} = 0.6\ h^{-1}$ for Passive House "Premium"), achieving this proved challenging. First, the prototype's high form factor (the ratio of external envelope surface area to internal volume) negatively impacted airtightness, as smaller buildings generally present greater difficulties in attaining low infiltration rates. Second, the integration of the hydrogen chamber within the thermal envelope added complexity to maintaining airtightness, see in Fig. 3. As the container housing the hydrogen installation must comply with the ATEX Directive, two automatically openable emergency extractors were installed in the lateral wall of the hydrogen room, oriented southwards, as shown in the module layout in Fig. 1. During the initial blower door tests, conducted in "cruise mode" at a constant pressure of 50 Pa, thermal imaging revealed that the main air leaks occurred around the extractors (see Fig. 4). After improving the external sealing of the openable door, the final blower door test indicated an average air change rate of 0.98 h^{-1} at 50 Pa, slightly below the Passivhaus "Low Energy Building" threshold and well below the maximum value permitted by the Spanish Building Code (see Table 4). Overall, this result is substantially lower than the air change rates measured in conventional container units, which range from 9.0 to 25.3 h^{-1} at 50 Pa [35].

Regarding the impact of this infiltration level on the prototype performance, Guillén-Lambea et al. [36] demonstrated that in warm climates the reduced indoor-outdoor temperature gradient leads to lower

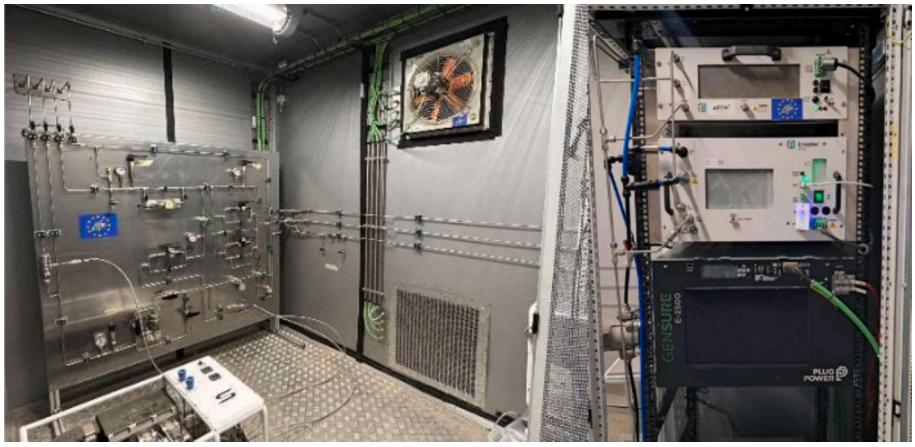

Fig. 3. Hydrogen room components: valve panel, compressor and emergency extractors (left) and the electrolyser and the fuel cell (right).

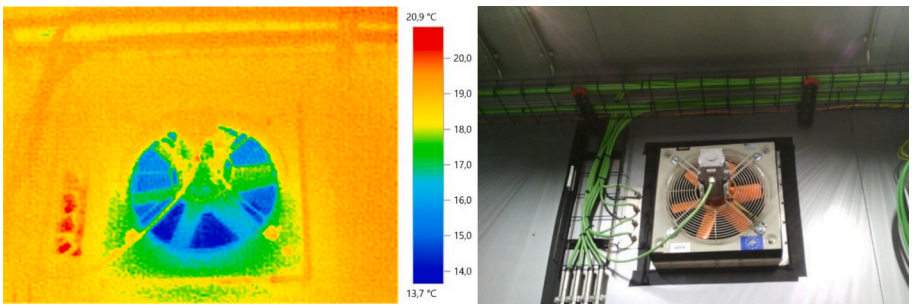

Fig. 4. Thermographic image of the upper extractor, captured during initial blower door testing at a constant pressure of 50 Pa.

pressure differences under normal operating conditions. Consequently, for a same infiltration measured at 50 Pa, the effective infiltration rate during real operation is significantly lower for warm climate compared to cold climate. The study reported that, under warm-climate conditions, a building with $n_{50} \approx 1\ h^{-1}$ may exhibit energy losses comparable to those of a colder-climate building with $n_{50} \approx 0.6\ h^{-1}$. Additionally, this level of airtightness does not significantly compromise the effective operation of a mechanical ventilation system with heat recovery.

Finally, it is worth noting that when the airtightness is expressed per unit of building envelope area (m^2), the resulting value is $q_{E50} = 0.5\ m^3/m^2.h$, which falls below the strictest requirements for Classic, Plus and Premium Passivhaus buildings.

3.2. Indoor Air Conditions

In this section we present the indoor air conditions measured in the ZEM prototype during the first demonstration at the Sapper Battalion I, in Zaragoza (Spain). The monitored parameters include indoor air temperature, relative humidity, CO_2 concentration, surface temperature of interior walls and vertical air temperature gradients at 0.2 and 1.5 m heights. Results are first presented for the entire monitoring year, followed by a detailed analysis of the weeks with the coldest and warmest outdoor temperatures.

3.2.1. One-year period

This section presents data collected between 1 September 2023 to 31 August 2024, during which the operation of the module was stable and fully automated. Graphs illustrate the temporal evolution of environmental conditions across the different spaces within the ZEM module, as measured by the sensors described in Fig. 1 and Table 3.

Fig. 5 compares daily averaged outdoor and indoor air temperatures. The largest differences occurred in December, when indoor conditions ranged between 18.7 °C (19-dec., room 3) and 27.3 °C (29-dec, room 1) depending on the day and the room. In May and June, as outdoor temperatures increased, the module maintained indoor conditions below 25 °C, in all the rooms. However, during July, when external conditions became more severe, the prototype was unable to sustain fully comfortable conditions, with peaks reaching approximately 32 °C in rooms MR2 and MR3. As discussed in Section 3.2.3, overheating occurred during heatwaves in Zaragoza and can be attributed to the fact that the ZEM prototype was originally designed for deployment in Antarctica and therefore required several adaptations to operate effectively in hot climates.

Overall, the average indoor temperature (calculated as the mean of T_{R1}, T_{R2}, T_{R3} and T_w) was 22.8 °C during the winter period and 25.2 °C during the summer period. These values fall within the comfort range recommended by both the Spanish regulation [37] and the EN 16798–1 standard [38]. They are also consistent with the Passivhaus design criteria adopted for the ZEM module, which assume indoor

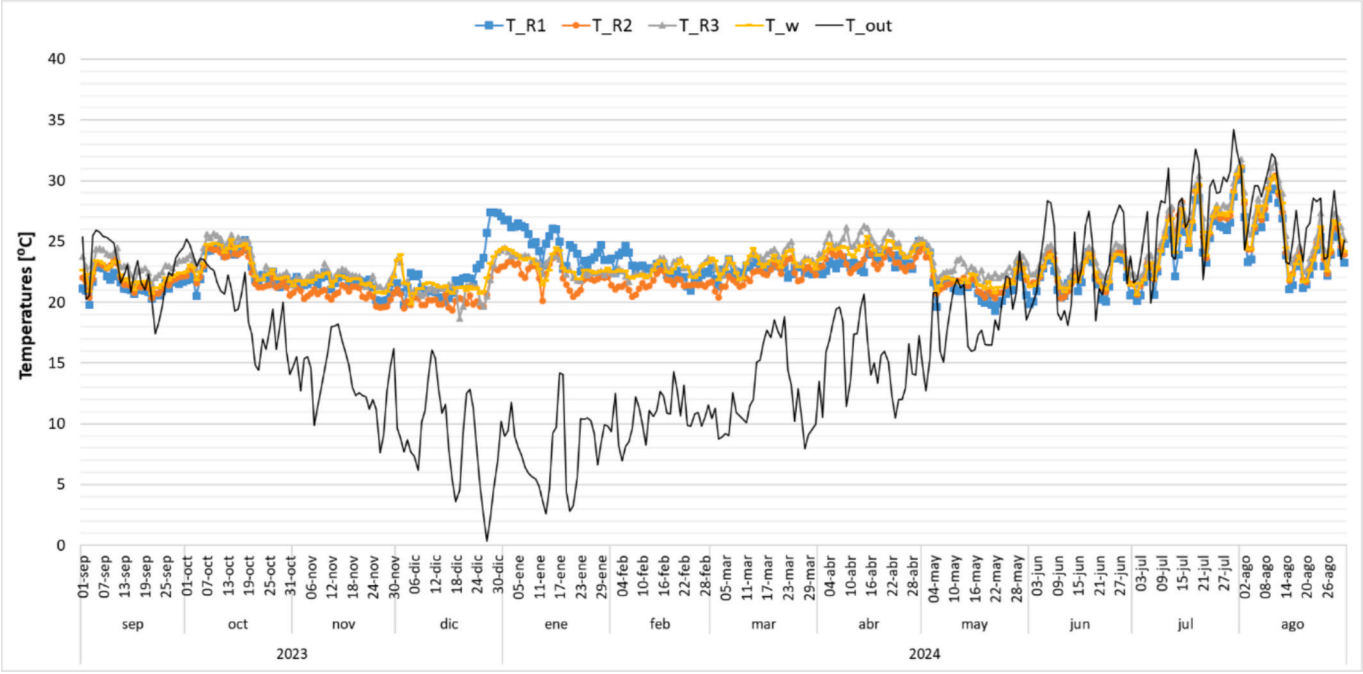

Fig. 5. Comparison of daily-averaged outdoor and indoor air temperatures within the ZEM prototype over the monitoring year.

temperatures of 20 and 25 °C for heating and cooling calculations, respectively. The slightly higher temperatures recorded in winter can be attributed to users behaviour, as occupants frequently increased the thermostat set-point, in some cases up to 24 °C.

When considering the rooms individually, MR2 was generally the coldest, except in summer when MR1 was slightly cooler. As shown in Fig. 1, MR2 serves as the entrance module of the prototype, containing the only accessible door, which was frequently opened due to the turnover of soldiers using the space. In addition, both the window and glazed-door of MR2 are north-facing, resulting in reduced solar gains during the winter months.

By contrast, MR3 was the warmest room for most of the year, except in December and January when an anomalous situation occurred and MR1 exhibited unusually high temperatures (see Section 3.2.2 for further details). The east–southeast orientation of the MR3 window, combined with the absence of shading elements or adjacent buildings, resulted in consistently high solar gains throughout the year.

The central core zone (T_w) displayed the most stable and comfortable temperatures. This corridor area received pre-conditioned air from the habitable rooms, which was then extracted towards the heat recovery unit located in the facility room. Moreover, this central zone is entirely internal, therefore free from thermal losses through the envelope.

Interestingly, MR1 recorded the lowest temperatures in summer and the highest in winter. This behaviour is attributable to its proximity to the facility room (see Fig. 1), where the PKOM unit is located, resulting in shorter air-conditioned ducts than those serving the other rooms. These temperature differences initially suggested a possible imbalance in airflow regulation among the habitable rooms. However, verification confirmed that the adjustment was correct. The main issue identified was the lack of insulation in the air ducts, which caused the conditioned air reaching MR3, i.e., the room furthest from the PKOM unit, to differ by several degrees from the supply air at the machine outlet.

Fig. 6 shows the temporal evolution of internal wall temperatures in the three habitable rooms (MR1, MR2 and MR3), compared with the outdoor temperature. By examining Fig. 5 and Fig. 6 together, it can be observed that indoor air temperatures and interior wall surface temperatures in each room follow almost identical trends. The average differences between the two over the entire monitoring period were 0.002, 0.342 and 0.595 °C in MR1, MR2 and MR3, respectively. These minimal differences highlight the strong performance of the ZEM prototype in terms of insulation and thermal comfort, avoiding the "cold wall" effect and fully complying the Passivhaus criterion, which recommends that interior surface temperatures do not fall more than 4.2 K below the operative indoor temperature [33].

Another parameter relevant to thermal comfort is vertical temperature stratification, commonly referred to as "cold feet" effect, which is often associated with thermal dissatisfaction. International standards for thermal environment, such as ISO 7730 [39] and ASHRAE 55 [40], recommend that for seated occupants the temperature difference between the head and ankle levels should not exceed 3 °C (5.4°F) to ensure comfort. Although these standards are widely applied, several studies, such as [41], suggest that vertical gradients of up to 8 K/m can be tolerated without causing discomfort. In contrast, the Passivhaus standard sets a stricter limit, with a maximum allowable temperature stratification of 2 °C between the head and feet of a seated person [33,42].

In this study, two sensors were installed in MR3 at 0.2 and 1.5 m heights, adjacent to the desk where a seated person worked ($T_{R3\_1.5}$ and $T_{R3\_0.2}$, see section 2.2.2). Fig. 7 depicts the monthly-averaged trends of these temperatures over the entire monitoring year. The mean temperature difference between 0.2 and 1.5 m height was 1.56 °C, indicating a nearly homogeneous vertical temperature distribution and confirming that the "cold feet" effect was negligible.

Fig. 8 shows the temporal evolution of the relative humidity in MR2, MR3 and the central core zone (RH_w) of the ZEM prototype. As can be observed, the three sensors recorded similar values and exhibited the same trends throughout the monitoring period, highlighting the homogeneity of indoor conditions. Relative humidity generally remained between 30 and 70 % for most of the year, which is slightly below the recommended range set by EN 16798–1 (25–60 %) [38]. However, values below 25 % were observed during the winter months, when outdoor air was cold and saturated in water vapour, and again in April 2024. Although the HVAC system includes enthalpy recovery, this was insufficient to prevent relative humidity from dropping sharply when incoming air is heated.

Concerning air quality, Fig. 9 presents the daily-average values of CO_2 concentration in MR2 (entrance room) and MR3 (office room). Although indoor CO_2 concentration alone does not provide a

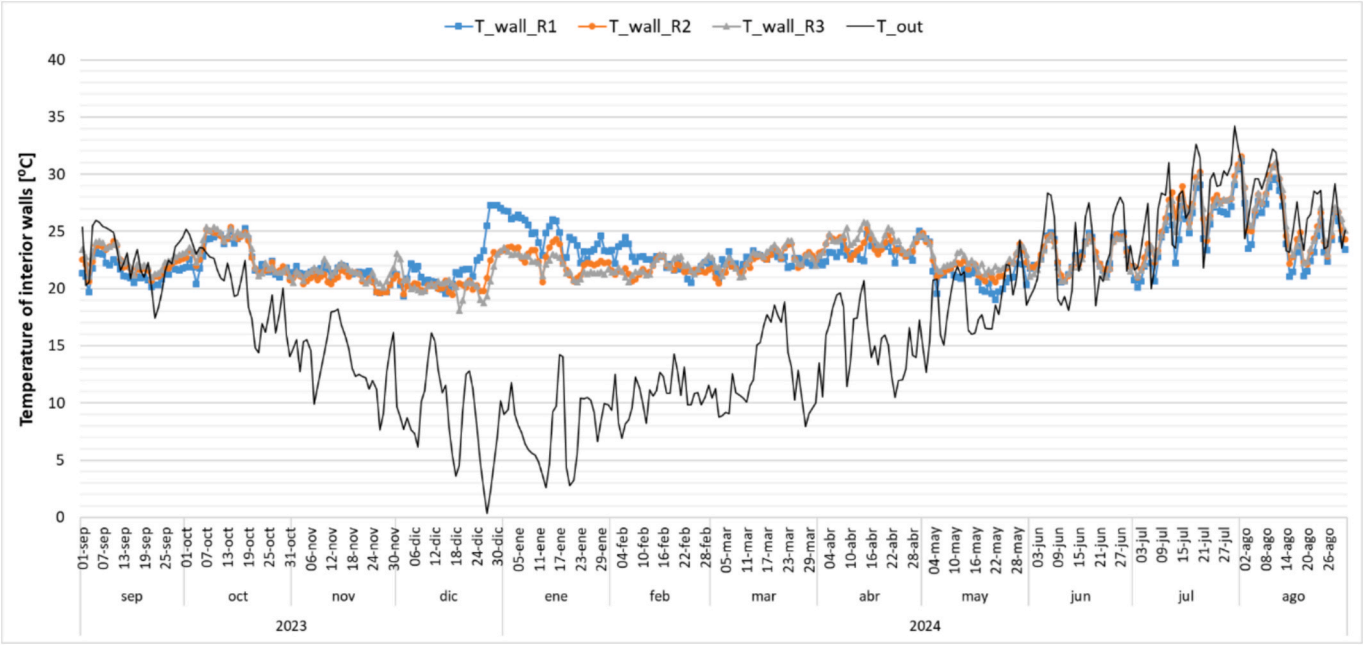

Fig. 6. Comparison of daily-averaged outdoor air temperature and interior wall temperatures in rooms 1 to 3 over the monitoring year.

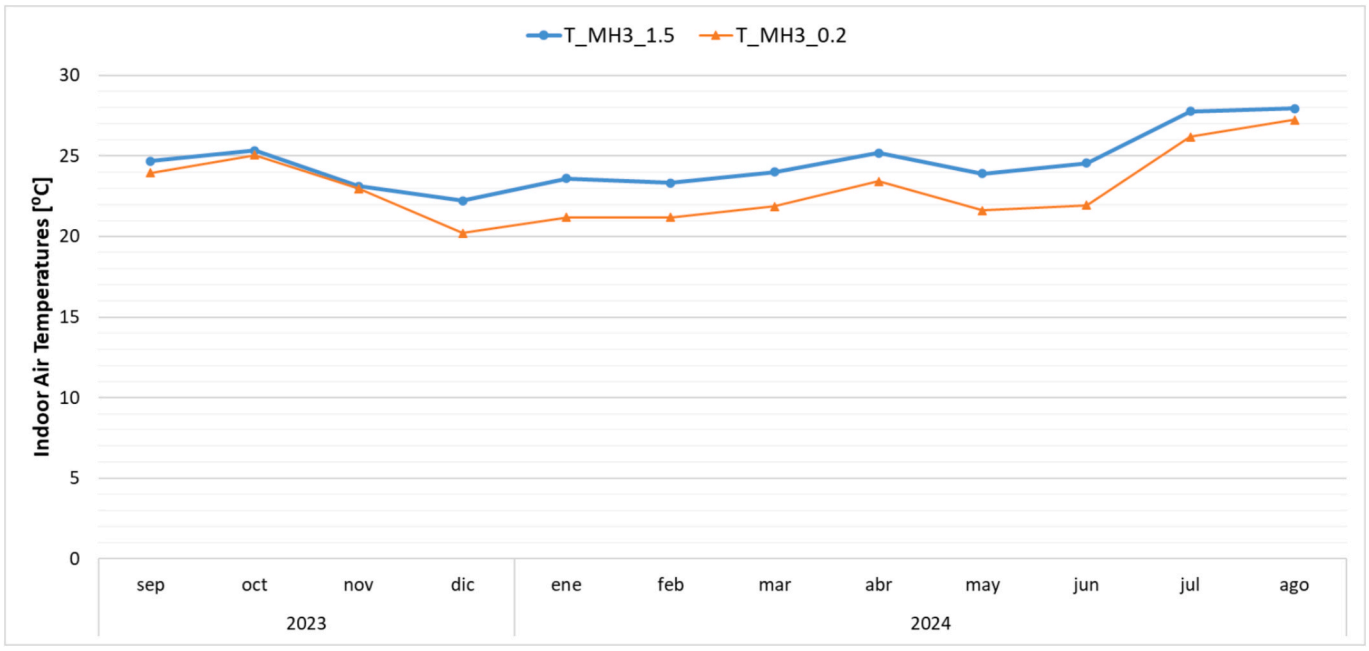

Fig. 7. Comparison of monthly-averaged air temperatures at 0.2 and 1.5 m heights, in room MR3 during the entire monitoring year.

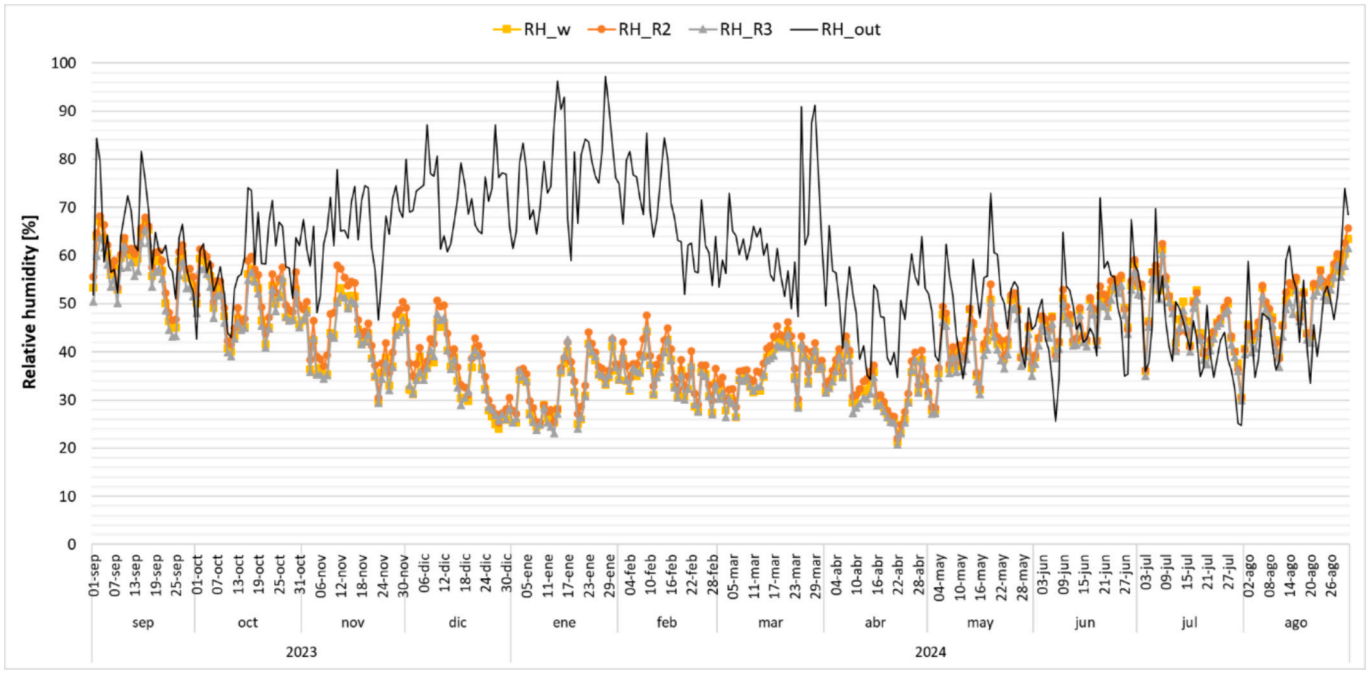

Fig. 8. Comparison of daily-averaged outdoor and indoor relative humidity within the ZEM prototype (rooms 2 and 3) over the monitoring year.

comprehensive assessment of Indoor Air Quality [43], it is widely used as an indicator of occupancy patterns and ventilation performance. As shown in Fig. 9, concentrations increased during working hours, when the module was occupied, and decreased during nights and weekends. Both rooms exhibited similar trends, with values remaining below 500 ppm on most days. Daily averages were consistently below 1000 ppm, indicating that the module was not overcrowded, and, more importantly, that the HVAC system ensured adequate air renewal, despite the absence of natural ventilation due to the non-openable windows.

To provide a more detailed analysis of thermal comfort within the ZEM prototype, the next two sections present the thermal conditions during the coldest and warmest weeks, respectively.

3.2.2. *Coldest week*

Fig. 10 shows hourly-averaged indoor air temperatures compared with outdoor temperatures during the coldest week of winter, from Monday 25 December to Sunday 31 December 2023. Overall, indoor temperatures were maintained at a very comfortable level, even during four consecutive days when the maximum outdoor temperature remained below 10 °C, with negative temperatures during nights. Throughout the week, temperatures measured in MR1 (T_{R1}) were higher than those in the other rooms, and it exhibited greater variability compared to T_{R2} and T_{R3}.

To understand this temperature behaviour, it is important to consider the operation and control of the HVAC system. As shown in

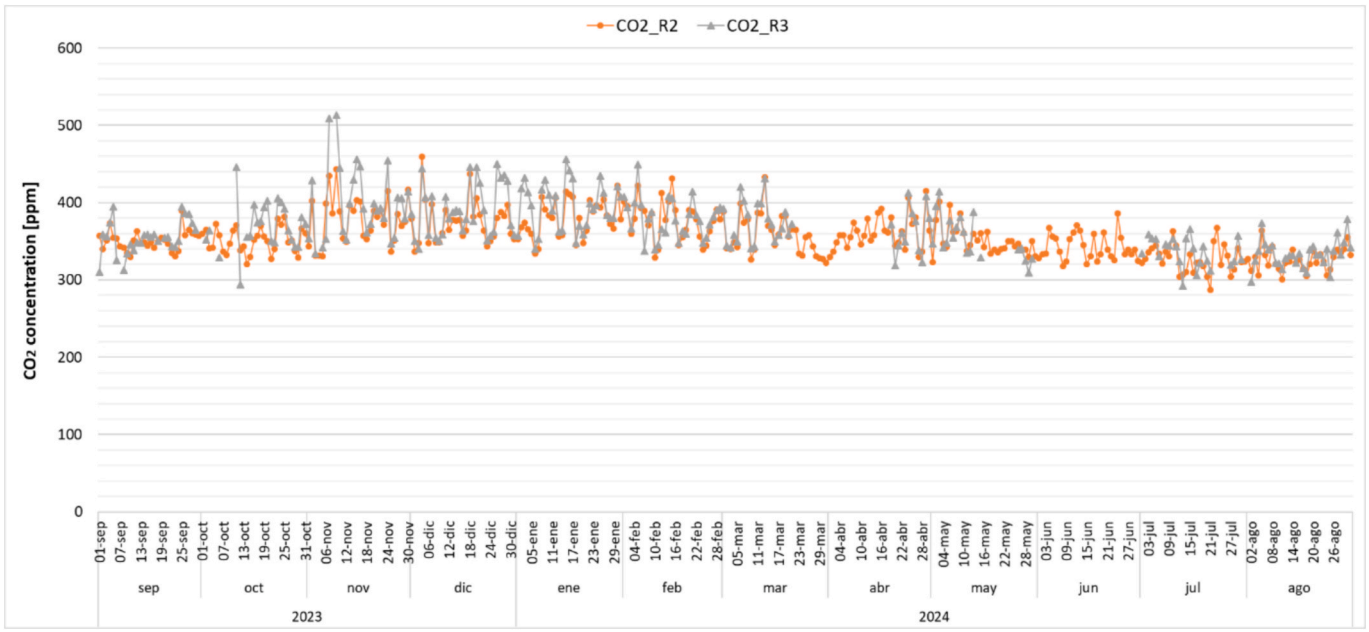

Fig. 9. Daily-averaged CO_2 concentration in the ZEM prototype (rooms 2 and 3) over the monitoring year.

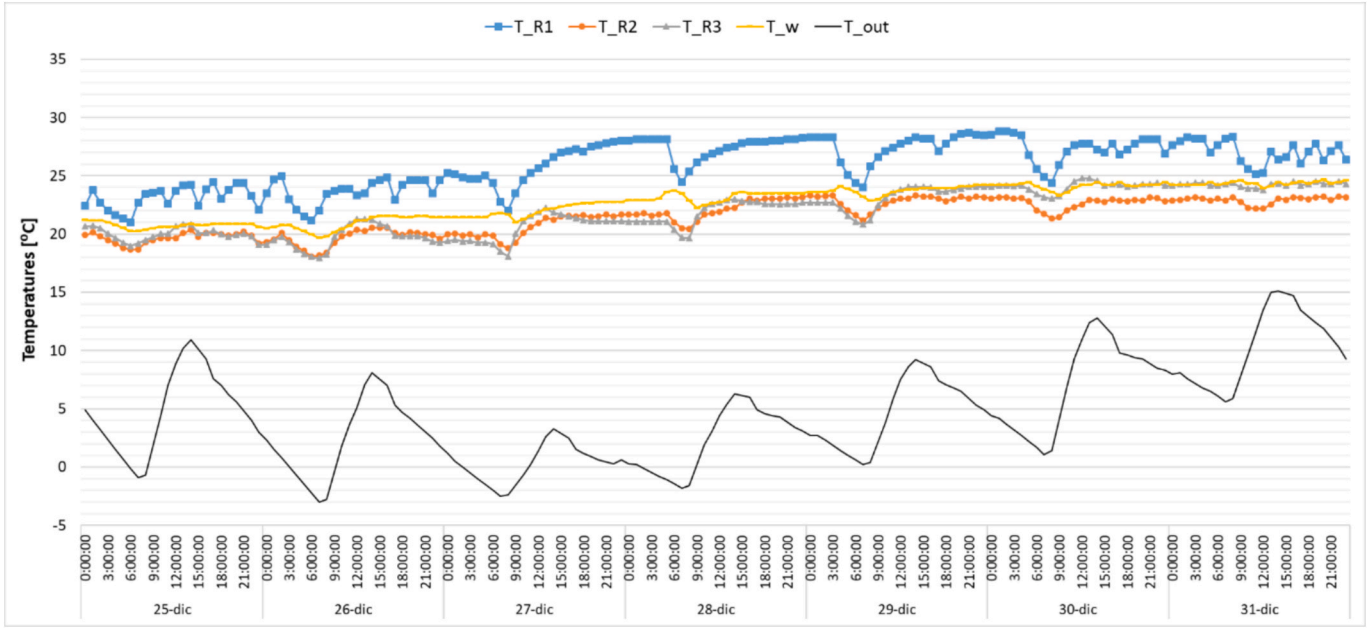

Fig. 10. Hourly-averaged outdoor and indoor air temperatures during winter 2023–24 coldest week.

Fig. 1, the HVAC unit is located in the facility room, adjacent to MR1. However, the HVAC system's temperature sensor is positioned as far as possible from the machine, in MR3 (see sensor T_{HVAC} in Fig. 1).

On 27 December 2023, users increased the set temperature from 20 °C up to 24 °C, in response to very low outdoor temperatures. During Wednesday 27 and Thursday 28 December, indoor temperatures gradually rose until the setpoint was reached in MR3. The HVAC unit then modulated the airflow with hysteresis to maintain the desired thermal comfort. It is noteworthy how the temperature behaviour differ among the three habitable rooms, particularly during the setpoint increase. Once the system stabilized, the differences in room temperatures became less pronounced. This observation reinforces the issue discussed in Section 3.2.1 regarding the lack of insulation in the conditioned air ducts, which causes T_{R1} to be higher (in winter) than the other rooms due to its proximity to the HVAC unit. Similarly, T_w was warmer than MR2 and MR3 due to heat losses through air ducts. T_{R3} exhibited the lowest temperatures for most of the week.

During this week, it can be clearly observed in Fig. 11 that users were present and working from Tuesday 26 to Friday 29, as indicated by the sharp increase in CO_2 concentration at 08:00 and the subsequent decrease around 16:00. A notable difference was observed between the two rooms, with CO_2 levels consistently higher in MR3 than in MR2. This can be attributed to the function of the rooms: MR2 serves as the entrance module, whereas MR3 is the office, occupied by two soldiers. Despite the noticeable increase in CO_2 concentrations during working hours, maximum hourly values remained below the 1000 ppm threshold (with the increment above outdoor CO_2 consistently below 500 ppm), indicating adequate ventilation rates throughout the week.

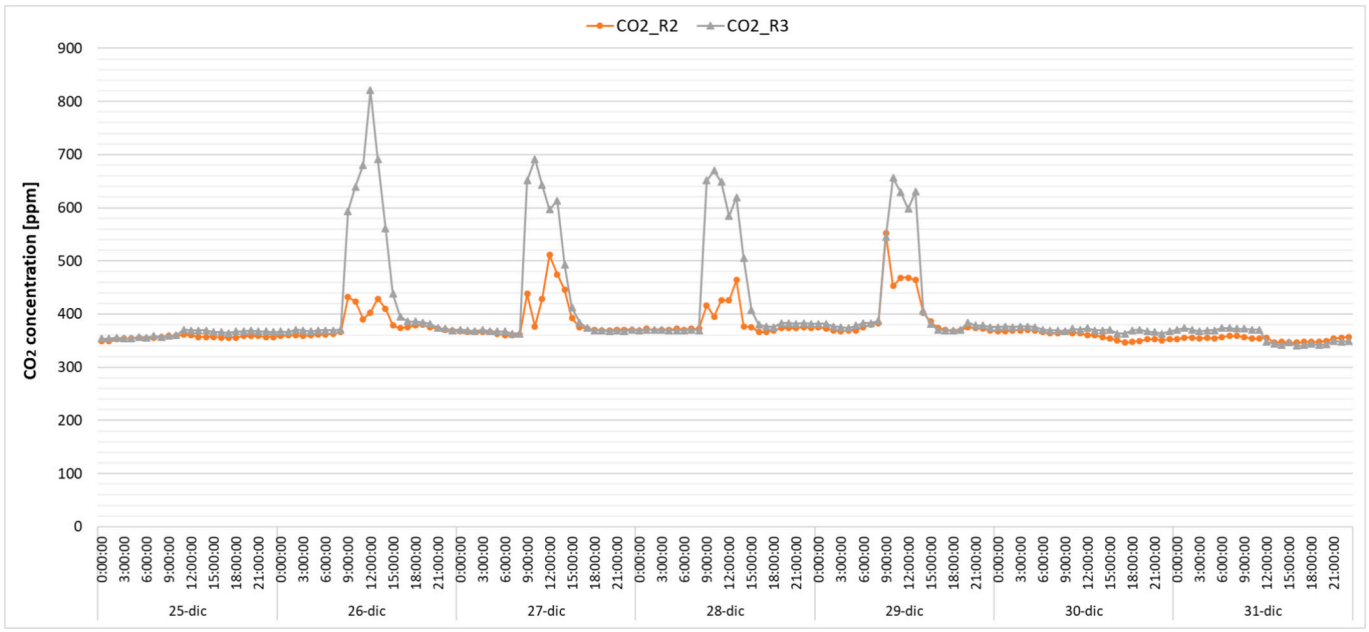

Fig. 11. Hourly-averaged CO_2 concentration in rooms 2 and 3 during the coldest week of winter.

Finally, Fig. 12 shows the temporal evolution of relative humidity, compared with outdoor conditions. The three sensors recorded very similar values, following the same daily trends. It can be observed that indoor relative humidity remained low throughout the week, ranging between 20 and 31 %. These low values can be attributed to the fully mechanically controlled ventilation system. Although the system includes enthalpy recovery, it was unable to maintain higher indoor humidity when the outdoor air is very cold and saturated with moisture, and heating demand is high.

3.2.3. *Warmest week*

This section presents data collected from Monday 5 to Sunday 11 August 2024, during a significant heatwave in Zaragoza. Maximum hourly-averaged outdoor temperatures reached up to 40 °C at 16:00 GMT + 00 (i.e., 18:00 local Spanish time), while minimum temperatures remained above 20 °C throughout the week, resulting in so-called "tropical nights". Fig. 13 shows the indoor air temperatures recorded within the ZEM prototype during this hot week. At the beginning of the week (Monday 5 August), indoor temperatures ranged from 23 to 29 °C, gradually increasing to 27–33 °C by Sunday 11 August.

Consistent with the analysis in Section 3.2.1, MR1 recorded the lowest temperatures throughout the week, while MR3 showed the highest values, particularly during the morning until midday, due to the east–southeast orientation of its window. By contrast, peak evening temperatures were observed in MR2, caused by heat gains through the glazed door, oriented west-northwest.

Despite HVAC unit operating at its maximum ventilation setting, it was unable to maintain fully comfortable indoor conditions. This was

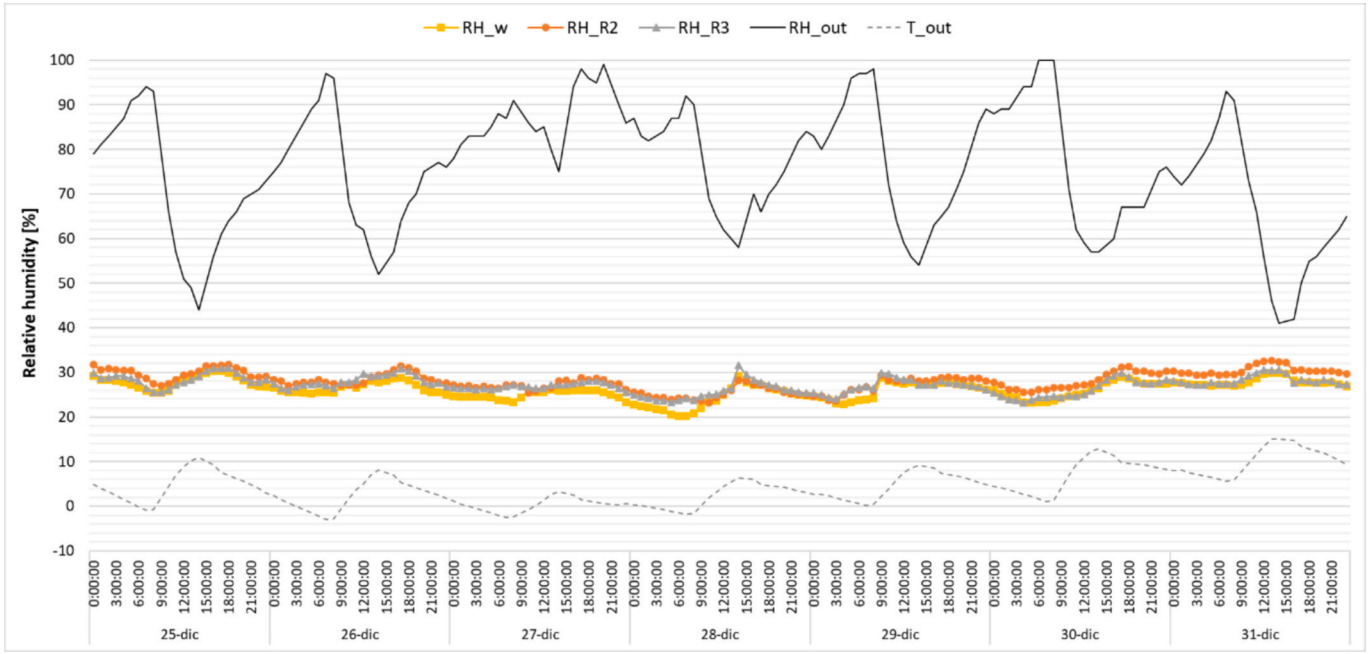

Fig. 12. Hourly-averaged relative humidity in the ZEM prototype during the coldest week of winter, compared to outdoor conditions.

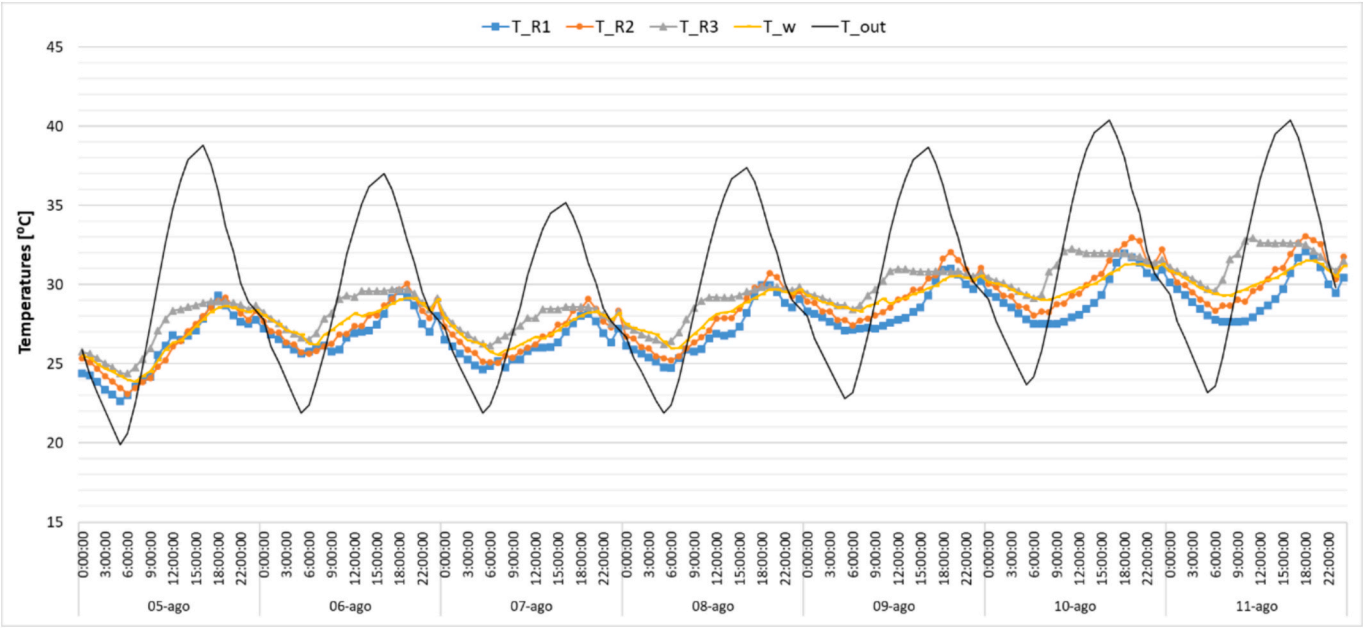

Fig. 13. Hourly-averaged outdoor and indoor air temperatures during the warmest week of summer 2024.

primarily due to several factors:

- Absence of shading devices: No shading is required for the ZEM deployment in the Antarctica. However, the demonstration in Zaragoza exposed the module to extreme summer conditions. Although additional shading elements for the windows and door had been planned, they were not implemented during the monitoring period, resulting in solar gains significantly higher than anticipated.
- Non-openable windows: The three windows are fixed, as required by design specifications for Antarctica deployment. However, in Zaragoza's hot summer climate, this prevented the use of natural nighttime ventilation and hindered the dissipation of accumulated heat. As shown in Fig. 13, indoor temperatures remained consistently higher than outdoor temperatures during the night, highlighting the cooling potential. The free-cooling mode of the PKOM unit provided only a limited airflow compared with what natural ventilation could have achieved.
- Limited cooling capacity: The air-conditioning system, which operates solely through ventilation, proved insufficient to counteract the extreme heatwave conditions.
- Additional internal loads: Despite its limited usable floor area, the ZEM module housed several appliances contributing to unwanted internal gains. These included a refrigerator, equipment related to the hydrogen cycle (compressor, electrolyzer and fuel cell), as well as various electronic devices in the facility room, all of which further increased cooling demand during summer. In particular, the electrolyzer and hydrogen compressor operated intensively during this period, when renewable energy production was high and surplus electricity was converted into hydrogen for storage.

Collectively, these factors caused substantial overheating of the ZEM prototype, with indoor air temperatures exceeding 25 °C for 1055 h over the monitored year (12.1 %). This overheating represents the main limitation of the prototype under extreme summer conditions. While the performance is considered reasonable, further mitigation measures—such as shading devices—are feasible and are currently implemented and under monitoring.

Regarding CO_2 concentrations, values remained low throughout the warmest week, as the HVAC system operated at its maximum ventilation rate. Fig. 14 illustrates the hourly-averaged CO_2 levels, showing that even during periods of higher occupancy, concentrations remained well below 550 ppm. On Friday 9 August, the reduced time spent indoors by soldiers (due to the elevated indoor temperatures) also contributed to the lower CO_2 levels observed that day.

Fig. 15 presents the hourly-averaged relative humidity recorded in MR2, MR3, and the central core zone (RH_w) during the warmest week. Compared to winter, relative humidity values exhibited greater variability, reflecting the larger temperature gradients characteristics of summer conditions. Nevertheless, indoor relative humidity was generally maintained within the acceptable range of 30–60 %. The lowest values were observed during afternoons and nights when the prototype was unoccupied (hence lacking moisture gains from human activity) and when both outdoor and indoor temperatures were higher.

3.2.4. *User interviews*

This section summarises the main findings from interviews conducted with three of the four soldiers who worked in the ZEM module during the demonstration period. The interviews were conducted in September 2024, following the completion of the monitoring campaign, and took the form of an open discussion involving the three soldiers and the three authors of this study. The discussion addressed qualitative aspects related to thermal comfort in both summer and winter, perceived cold-floor effects, air draughts, insufficient ventilation, unpleasant odours or humidity, acoustic and visual comfort, and the overall experience of working in the passive container module compared with conventional Army containers units.

During winter, users consistently reported a comfortable environment. They described the indoor conditions as pleasant and warm in the mornings, without experiencing draughts or the "cold feet" effect. They also confirmed the absence of "stale air" sensations, despite the low relative humidity values measured. No symptoms typically associated with dry air (e.g., throat or nasal dryness, eye irritation) were mentioned. These statements are consistent with the monitoring data, which indicated stable indoor temperatures and acceptable air quality during the coldest periods.

In contrast, during summer users reported discomfort due to excessive heat and humidity, describing the environment as sticky and increasingly stifling throughout the day. They also highlighted significant temperature differences between rooms, estimating up to 10 °C variation, which corresponds with the sensor data showing higher

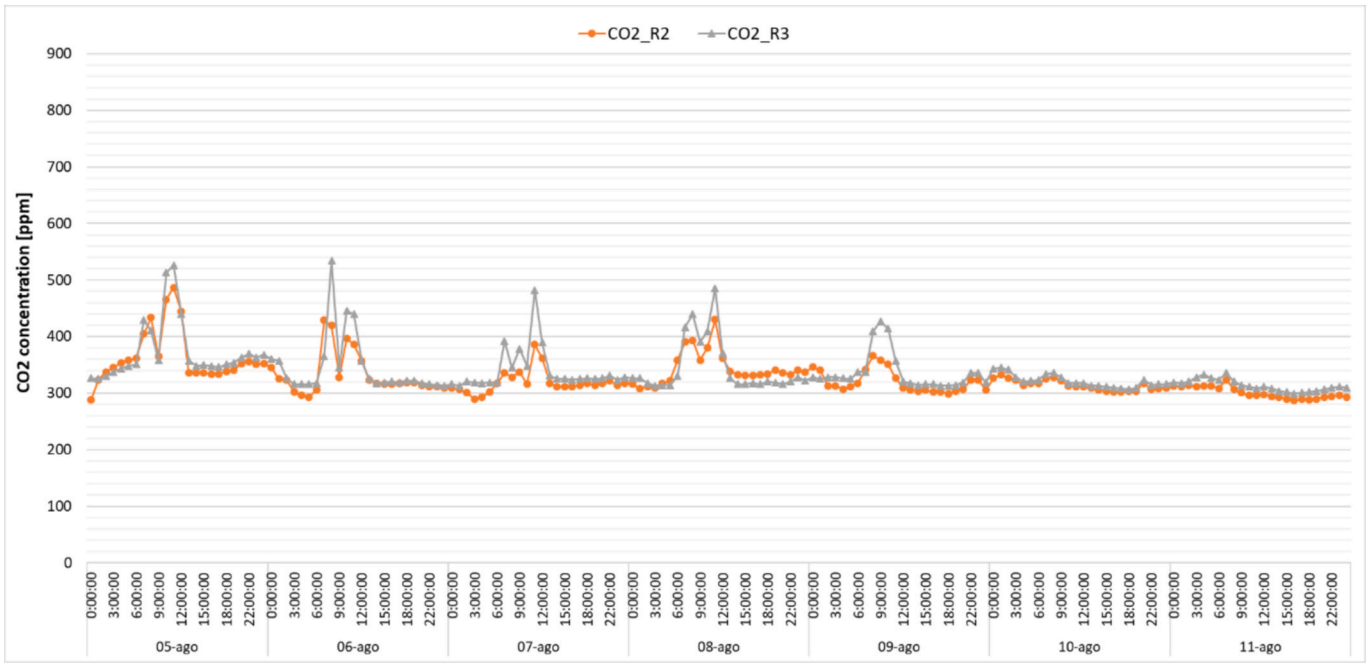

Fig. 14. Hourly-averaged CO_2 concentration in rooms 2 and 3 during the warmest week of summer 2024.

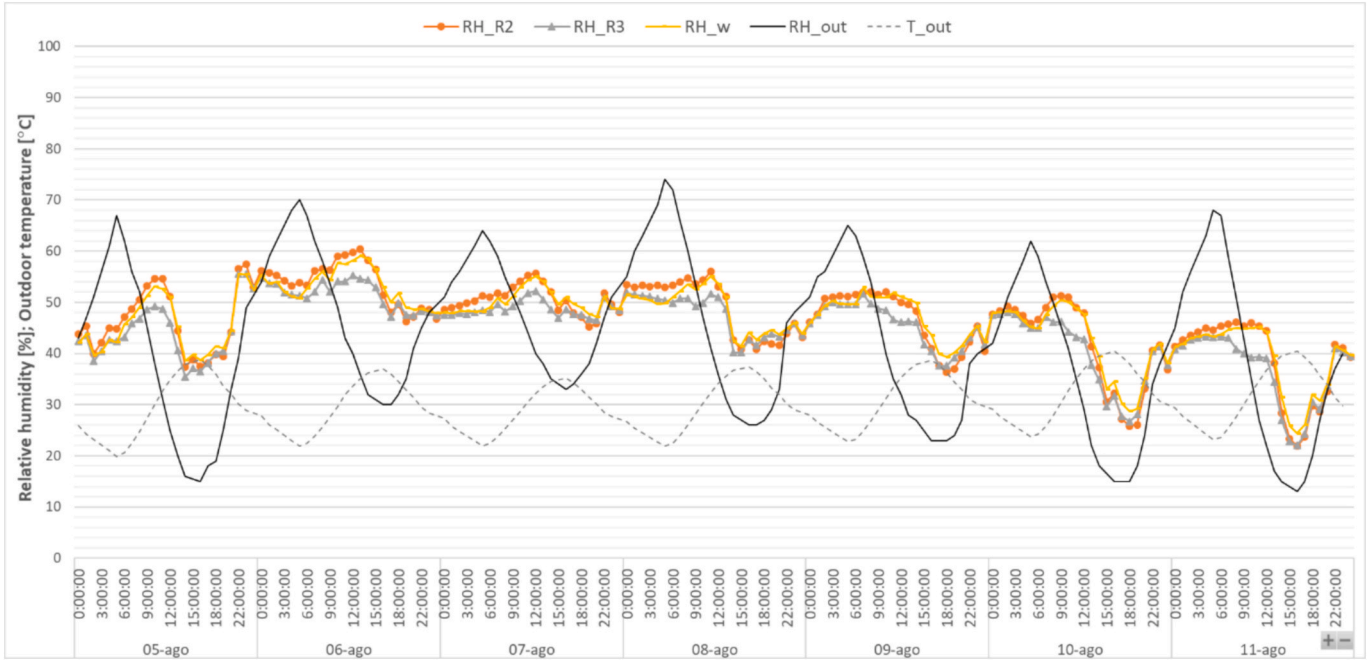

Fig. 15. Hourly-averaged relative humidity during the warmest week, compared to outdoor conditions.

overheating in MR3 and lower values in MR1.

Overall, the subjective feedback from the occupants corroborates the quantitative results presented in Sections 3.2.2 and 3.2.3, confirming satisfactory thermal comfort in winter and marked overheating during the heatwave in summer.

3.3. Energy consumption results

For the purpose of analysing energy consumption per unit area, the Treated Floor Area (TFA) was used, as defined by the Passive House Planning Package (PHPP) manual [44]. The THA corresponds to the net floor area of a building that is heated or air-conditioned, and is approximately equivalent to the gross internal floor area, excluding areas occupied by internal walls. Weighting factors are applied depending on room use: 100 % or 60 %. In the case of the ZEM prototype, the three living modules, together with the corridor, shower and toilets are weighted at 100 %, while the facility and hydrogen container is weighted at 60 %. This results in a total TFA of 56.8 m^2.

Table 5 presents the disaggregated energy consumption of the PKOM4 unit (see Section 2.1 for details) for ventilation, heating, cooling and DHW, recorded over the monitoring period from 1 September 2023 to 31 August 2024 (one full year). Cooling represented the largest share, accounting for 54 % of the total energy consumed by the HVAC and DHW system. This outcome was expected, given the climatic conditions

in Zaragoza, where extreme summer temperatures can reach up to 44 °C during heatwaves. For illustration, during the warmest week (5–11 August), the cooling energy consumption amounted to 106 kWh. With a seasonal coefficient of performance (SCOP) of 2.18, obtained from the one-year measurement by the PKOM unit, this corresponds to a cooling demand of 231 kWh, equivalents to 4.1 kWh/m^2 in a single week.

Ventilation represented the second largest share of demand, which is consistent with the system configuration, as air conditioning was provided exclusively through mechanical ventilation.

When considering only the energy consumption for heating and cooling, the ZEM prototype reached a total of 33.9 kWh/m^2 per year, representing an 87 % reduction compared with the values reported for conventional containers deployed at the Miguel de Cervantes base in Lebanon [8]. Although the two cases correspond to different climatic contexts, Zaragoza presents a more demanding scenario in terms of total heating and cooling degree days (2694 °C·days) compared to Beirut (1881 °C·days), according to data obtained from the BizEE Degree Days database (DegreeDays.net), recommended by ASHRAE. Given that Zaragoza exhibits higher total degree days, a direct comparison with a conventional container operating under the same climatic conditions would likely result in an even greater relative reduction. This comparison suggests that the substantial reduction in energy use is primarily associated with the enhanced envelope performance, higher insulation levels, improved airtightness, and the efficiency of the installed systems, rather than being solely explained by climatic differences. The reduction is particularly significant during winter, consistent with the fact that the ZEM prototype was originally designed for deployment in polar climates.

Under summer conditions, cooling demand could be further reduced through the incorporation of external shading devices and improved insulation of the air-distribution ducts, measures that are currently being implemented and monitored. It should be emphasised that the reported 87 % reduction refers strictly to monitored annual heating and cooling energy consumption. While thermal comfort and energy performance are interrelated, they represent distinct evaluation criteria. Although periods of summer overheating were observed under the severe climatic conditions of Zaragoza, these do not undermine the measured reduction in HVAC energy demand. Rather, they highlight opportunities for additional passive optimisation to enhance summer comfort while preserving the low energy consumption achieved.

4. Lessons learnt and conclusions

This paper presented the design, implementation and experimental assessment of the so-called “Zero Energy Module” (ZEM), a transportable and demountable prototype based on shipping containers. The primary objective was to demonstrate that very high energy efficiency and adequate indoor environmental quality can be achieved in container-based constructions by combining Passivhaus design principles and highly efficient installations. The prototype was experimentally validated during a one-year monitoring campaign at a military base in Zaragoza, Spain. It should be noted that Zaragoza represents a semi-arid climate with very severe hot summers. While the prototype was originally designed for its deployment in Antarctica, Zaragoza climate provided a stringent test of its passive and energy-efficient design.

To clearly differentiate between empirically validated results and forward-looking design implications, the conclusions are structured into two categories: (i) those supported by measured performance data, and (ii) those derived from design characteristics or adaptation potential.

Table 5
Energy consumption of the ZEM prototype for HVAC and DHW, in kWh, during one year of monitoring.

	Ventilation	Heating	Cooling	DHW	Total
Energy Consumption [kWh]	907	314	1613	108	2942
Energy Consumption [kWh/m^2]	16.0	5.5	28.4	1.9	51.8

4.1. Conclusions Supported by Measured Performance Data

- **A substantial reduction in heating and cooling energy demand:** The measured annual energy consumption for heating and cooling was 33.9 kWh/m^2 per year, which is more than 87 % lower than that of conventional container units previously monitored at military bases. This reduction was achieved by applying the Passivhaus standard, which involves high and continuous insulation levels, reduced thermal bridges, improved airtightness, and efficient HVAC systems.
- **Airtightness:** Blower door testing confirmed an airtightness level of 0.98 h^{-1} at 50 Pa, which complies with the Passivhaus 'Low Energy Demand Building' criterion. This was achieved despite the additional challenges introduced by integrating an ATEX-compliant hydrogen room within the thermal envelope.
- **Thermal comfort**: Interior surface temperature measurements showed a minimal difference between air and wall temperatures, confirming the absence of cold-wall effects. Vertical temperature stratification remained well below 2 °C, indicating homogeneous indoor thermal conditions.
- **Stable winter comfort conditions:** During the coldest monitored week, indoor temperatures remained within a comfortable range, despite sub-zero outdoor conditions. This was achieved through the use of a compact aerothermal unit combined with an enthalpy heat recovery ventilation system. These results demonstrate the system's effective performance in such climatic conditions. However, the results also suggest that controlled humidification could further improve comfort during periods of very low outdoor temperatures.
- **Controlled indoor air renovation:** Throughout the year, daily average CO_2 levels remained below 1000 ppm, generally falling below 500 ppm after occupancy peaks. This confirms that, despite the absence of operable windows, mechanical ventilation with heat recovery ensured sufficient air renewal.
- **Overheating during extreme summer heatwaves:** Measured data show that indoor temperatures exceeded 25 °C for 1055 h (12.1 % of the monitored year), with peaks above 30 °C occurring during heatwaves. These results confirm that the current configuration is not fully adapted to severe hot summer conditions, as initially designed for polar conditions.
- **Sensitivity to system details and operational factors**: Monitoring revealed temperature differences between rooms attributable to uninsulated air-distribution ducts and HVAC operation and control strategies. These findings demonstrate that relatively minor technical details can exert a significant influence on thermal performance in highly efficient buildings. Furthermore, the results indicate that user behaviour plays a more pronounced role in overall performance than in conventional constructions.

4.2. Conclusions Based on Design Features and Future Adaptation Potential

The following conclusions derive from the underlying design principles of the prototype, its scalability and its potential improvements for further optimisation.

- **Replicability of the high-performance envelope concept**: The combination of continuous external insulation, minimised thermal bridges, and high airtightness defines a transferable design pathway for container-based constructions. While the present prototype has been experimentally validated, implementation in other climatic contexts or at larger scales would require site-specific adaptation and optimisation.

- **Energy production and storage outside the thermal envelope**: The integration of the ATEX hydrogen room within the thermal envelope introduced additional constraints, including increased internal loads, acoustic impacts, and challenges related to airtightness. Locating energy production and storage systems outside the conditioned volume would simplify compliance with stringent envelope performance targets in future designs.
- **Adaptability to different climatic contexts:** Although originally designed for Antarctic deployment, the prototype can be adapted to warmer climates through the incorporation of external shading devices, improved insulation of air-ducts and enhanced passive cooling strategies. These measures are technically feasible and are currently being implemented and monitored.
- **Potential improvement of summer performance:** The absence of shading devices and natural night-time ventilation contributed significantly to overheating during the Zaragoza monitoring period. Design analysis and simulations suggest that integrating external shading and enabling night-time cooling through opening windows would reduce peak indoor temperatures. However, the magnitude of this improvement remains to be experimentally validated.
- **Suitability for autonomous and remote applications:** Integrating high-efficiency systems with renewable generation and hydrogen storage demonstrates the conceptual feasibility of energy autonomy in remote military or humanitarian contexts. Although the demand-side performance has been validated, achieving a full annual net-zero balance under diverse field conditions requires further investigation.
- **Broader applicability beyond military contexts:** The ZEM concept can be easily adapted for a variety of temporary and semi-permanent applications, such as humanitarian aid, emergency housing, temporary schools, and healthcare facilities.

Overall, this study shows that buildings based on shipping containers can form the basis of a new generation of low- and nearly zero-energy modular constructions. Prioritising energy efficiency as the primary design principle, alongside the integration of renewable energy and efficient systems, establishes a robust approach to reducing energy demand, CO_2 emissions, and operational costs in remote and temporary building applications under various climatic conditions.

Declaration of Generative AI and AI-assisted technologies in the writing process

During the preparation of this work, the authors used ChatGPT (OpenAI) to assist in improving the clarity, grammar, and overall readability of the manuscript. After using this tool, the authors reviewed and edited the content as needed and take full responsibility for the content of the published article.

CRediT authorship contribution statement

Adeline Rezeau: Writing – original draft, Visualization, Methodology, Investigation, Formal analysis, Data curation, Conceptualization. **Beatriz Rodríguez-Soria:** Writing – review & editing, Supervision, Project administration, Methodology, Investigation, Funding acquisition, Formal analysis, Conceptualization. **Miguel Ángel García-García:** Writing – review & editing, Methodology, Investigation.

Declaration of competing interest

The authors declare that they have no known competing financial interests or personal relationships that could have appeared to influence the work reported in this paper.

Acknowledgment

This project has received funding from the LIFE program of the European Commission [grant ref. LIFE19 CCM/ES/001327]. We express our gratitude to the Aragon Regiment – Sapper Battalion I for their support in testing and providing feedback on the module's operation and to Orkli for their assistance with the operation of the PKMO4 machine.

Appendix

Table A1
Characteristics of the building assembly used for horizontal roof and floor, and vertical walls (materials listed from exterior to interior).

Material	Thickness [mm]	Thermal conductivity [W/mK]	Thermal resistance [m^2K/W]	U-value [W/m^2K]
Stainless steel	1	17	–	0.072
XPS	300	0.035	8.57	
Stainless steel	1	17	–	
Air chamber	5	0.040	0.13	
Lacquered steel	1	80	–	
Mineral wool	100	0.037	2.70	
Lacquered steel	2	80	–	
Mineral wool	100	0.037	2.70	
Lacquered steel	1	80	–	
Total	511		14.10	

Thermal resistance of steel-based components (< 0.0001 m^2K/W) is negligible in the final U-value of the walls.

Data availability

Data will be made available on request.

References

[1] Y. Wang, L. Wang, E. Long, S. Deng, An experimental study on the indoor thermal environment in prefabricated houses in the subtropics, Energy Build. 127 (2016) 529–539, https://doi.org/10.1016/j.enbuild.2016.05.061.

[2] J. Shen, B. Copertaro, X. Zhang, J. Koke, P. Kaufmann, S. Krause, "Exploring the potential of climate-adaptive container building design under future climates scenarios in three different climate zones", Sustainability (Switzerland) 12 (1) (2020) https://doi.org/10.3390/SU12010108.

[3] J.A. Peña, K. Schuzer, "Design of Reusable Emergency Relief Housing Units Using General-Purpose Shipping Containers" [Online] Available: *Int. J. Eng. Res. Innov.* 4 (2) (2012).

[4] G. Zhang, S. Setunge, S. van Elmpt, Using shipping Containers to provide Temporary Housing in Post-disaster Recovery: Social Case Studies, Procedia Economics and Finance 18 (September) (2014) 618–625, https://doi.org/10.1016/s2212-5671(14)00983-6.

[5] A. Atmaca, N. Atmaca, Comparative life cycle energy and cost analysis of post-disaster temporary housings, Appl. Energy 171 (March) (2016) 429–443, https://doi.org/10.1016/j.apenergy.2016.03.058.

[6] C. Samaras, W.J. Nuttall, M. Bazilian, Energy and the military: Convergence of security, economic, and environmental decision-making, Energ. Strat. Rev. 26 (September) (2019) 100409, https://doi.org/10.1016/j.esr.2019.100409.

[7] J. L. Palés, "Transcript of General Palés' speech at the International Security Exhibition," *SICUR 2014: Technological Brokerage Event in Security*, 2014.

[8] B. Rodríguez-Soria, M. Á. García-García, and A. Rezeau, "Módulos Habitables de Consumo de Energía Casi Nulo para Bases Militares en Entornos NATO," *Ingenieros Politécnicos*, vol. 10, no. ISNN 2444-7757, pp. 44–53, 2023.

[9] B. Rodriguez-Soria, M.Á. García-García, A. Rezeau, Energy characterization of buildings in polar climate: Case study of Gabriel de Castilla Antarctic station, Energy Build. 308 (December) (2023) 2024, https://doi.org/10.1016/j.enbuild.2024.114028.

[10] A. Volkova, "Energy efficiency indicators for the heat supply sector," *ODYSSEE-MURE Policy brief*, no. October, 2024.

[11] Passive House Institute, "Criteria for Buildings. Passive House - EnerPHit - PHI Low Energy Building. Versión 10c," no. January, p. 131, 2023.

[12] "Directive (EU) 2024/1275 of the European Parliament and of the Council of 24 April 2024 on the energy performance of buildings," *Official Journal of the European Union*, vol. 1275, pp. 1–68, 2024.

[13] G.M. Elrayies, Thermal performance assessment of shipping container architecture in hot and humid climates, Int. J. Adv. Sci. Eng. Inf. Technol. 7 (4) (2017) 1114–1126, https://doi.org/10.18517/ijaseit.7.4.2235.

[14] B.B.F. da Costa, C.F.P. Silva, A.C.F. Maciel, H.D.P. Cusi, G. Maquera, A.N. Haddad, Simulation and Analysis of thermal Insulators Applied to Post-disaster Temporary Shelters in Tropical Countries, Designs (basel) 7 (3) (2023) 1–21, https://doi.org/10.3390/designs7030064.

[15] J. Koke, A. Schippmann, J. Shen, X. Zhang, P. Kaufmann, S. Krause, "Strategies of design concepts and energy systems for nearly zero-energy container buildings (NZECBs) in different climates", *Buildings* 11 (8) (2021) https://doi.org/10.3390/buildings11080364.

[16] H. Suo, X. Guan, S. Wu, Z. Fan, "Energy Performance Assessment of the Container Housing in Subtropical Region of China upon Future climate Scenarios", Energies (basel) 16 (1) (2023) https://doi.org/10.3390/en16010503.

[17] S. Schiavoni, S. Sambuco, A. Rotili, F. D'Alessandro, F. Fantauzzi, A nZEB housing structure derived from end of life containers: Energy, lighting and life cycle assessment, Build. Simul. 10 (2) (2017) 165–181, https://doi.org/10.1007/s12273-016-0329-9.

[18] D. Satola, A.B. Kristiansen, A. Houlihan-Wiberg, A. Gustavsen, T. Ma, R.Z. Wang, Comparative life cycle assessment of various energy efficiency designs of a container-based housing unit in China: a case study, Build. Environ. 186 (September) (2020), https://doi.org/10.1016/j.buildenv.2020.107358.

[19] C. Dara, C. Hachem-Vermette, G. Assefa, Life cycle assessment and life cycle costing of container-based single-family housing in Canada: a case study, Build. Environ. 163 (March) (2019), https://doi.org/10.1016/j.buildenv.2019.106332.

[20] C. Dara, C. Hachem-Vermette, Evaluation of low-impact modular housing using energy optimization and life cycle analysis, Energy Ecol. Environ. 4 (6) (2019) 286–299, https://doi.org/10.1007/s40974-019-00135-4.

[21] C. Dara, "Design Investigation of Container-based Residential buildings for improved Energy and Environmental Performance. Integrated Life Cycle Perspective,, University of Calgary, 2021.

[22] V. Tavares, N. Lacerda, F. Freire, Embodied energy and greenhouse gas emissions analysis of a prefabricated modular house: the 'Moby' case study, J. Clean. Prod. 212 (2019) 1044–1053, https://doi.org/10.1016/j.jclepro.2018.12.028.

[23] Y. Wei, et al., A multidimensional assessment of passive container houses: Energy, emissions, and economics, J. Build. Eng. 111 (July) (2025), https://doi.org/10.1016/j.jobe.2025.113507.

[24] A.B. Kristiansen, et al., Feasibility study of an off-grid container unit for industrial construction, Sustain. Cities Soc. 61 (June) (2020), https://doi.org/10.1016/j.scs.2020.102335.

[25] NATO standardization office, "NATO standard AJEPP 2 : Environmental best practice and standards for military camps in NATO operations," no. November, 2018.

[26] NATO standardization office, "NATO standard AJEPP-4: Joint NATO doctrine for environmental protection during NATO-led military activities. Edition B Version 1.," no. March, p. 30, 2018.

[27] "The Antarctic Treaty," in *Conference on Antarctica*, Washington D.C., USA, 1959, p. 53.

[28] Secretariat of the Antarctic Treaty, "Protocol on Environmental Protection to the Antarctic Treaty (the Madrid Protocol)," 1991.

[29] Gobierno de España, "Royal Decree 450/2022, of June 14, amending the Technical Building Code, approved by Royal Decree 314/2006, of March 17," *Boletín Oficial del Estado*, pp. 61561–61567, 2022.

[30] D. D'Agostino, S.T. Tzeiranaki, P. Zangheri, P. Bertoldi, Data on nearly zero energy buildings (NZEBs) projects and best practices in Europe, Data Brief 39 (2021), https://doi.org/10.1016/j.dib.2021.107641.

[31] Pichler, "Heat pump combination unit. Product description PKOM4." [Online]. Available: https://www.pichlerluft.at/heat-pump-combination-unit.html.

[32] International Organization for Standardization, "ISO 9972 Thermal performance of buildings - Determination of air permeability of buildings - Fan pressurization method," 2015.

[33] Passive House Institute, "Criteria for Buildings. Passive House - EnerPHit - PHI Low Energy Building. Versión 10c," no. January, p. 131, 2023.

[34] P.M. Congedo, C. Baglivo, D. D'Agostino, P.M. Albanese, Overview of EU building envelope energy requirement for climate neutrality, Renew. Sustain. Energy Rev. 202 (June) (2024) 114712, https://doi.org/10.1016/j.rser.2024.114712.

[35] A.M. Tanyer, A. Tavukcuoglu, M. Bekboliev, Assessing the airtightness performance of container houses in relation to its effect on energy efficiency, Build. Environ. 134 (1) (2018) 59–73, https://doi.org/10.1016/j.buildenv.2018.02.026.

[36] S. Guillén-Lambea, B. Rodríguez-Soria, J.M. Marín, Air infiltrations and energy demand for residential low energy buildings in warm climates, Renew. Sustain. Energy Rev. 116 (October) (2019), https://doi.org/10.1016/j.rser.2019.109469.

[37] BOE, "Real Decreto 1027/2007, de 20 de julio, por el que se aprueba el Reglamento de Instalaciones Térmicas en los Edificios.," 2007.

[38] European Norm, "EN 16798 -1 Energy performance of buildings. Ventilation for buildings. Part 1: Indoor environmental input parameteres for design and assessment of energy performance of buildings addressing indoor air quality, thermal environment, lighting and acoustics.," 2019.

[39] International Organization for Standardization, "ISO 7730 - Ergonomics of the thermal environment – analytical determination and interpretation of thermal comfort using calculation of the PMV and PPD indices and local thermal comfort criteria," 2025.

[40] ANSI/ASHRAE, "Standard 55 - Thermal Environmental Conditions for Human Occupancy," 2023.

[41] M. Möhlenkamp, M. Schmidt, M. Wesseling, A. Wick, I. Gores, D. Müller, Thermal comfort in environments with different vertical air temperature gradients, Indoor Air 29 (1) (2019) 101–111, https://doi.org/10.1111/ina.12512.

[42] PASSIPEDIA. The Passive House Resource, "Thermal comfort parameters." [Online]. Available: https://passipedia.org/basics/building_physics_-_basics/thermal_comfort/thermal_comfort_parameters.

[43] ASHRAE Board of Directors, "ASHRAE Position Document on Indoor Carbon Dioxide," p. 17, 2022.

[44] W. Feist et al., "PHPP Passive House Planning Package - version 10," Darmstadt, 2021.